

V. A. Pilipovich, V. L. Malevich,  
G. D. Ivlev, and V. V. Zhidkov

UDC 678.029.73:621.373.826

On the basis of a numerical solution of the Stefan problem, the dynamics of nanosecond laser annealing of silicon is investigated.

The annealing of ion-implanted semiconductor layers by nanosecond laser pulses has recently been investigated intensively. This problem has not only a great applied but also, in principle, a theoretical value since its study permits better understanding of the physics of the crystallization process as a whole.

Two nanosecond laser annealing mechanisms are known most, thermal and plasma. If it is assumed in the first model that restoration of the crystalline structure occurs after short-range melting and subsequent crystallization of the melt, then in the plasma model annealing is associated with the formation of a dense electron-hole plasma under the action of the laser pulse.

The temperature of a silicon surface under laser heating was measured by different methods in [1-6]. On the basis of the experiment data, deductions were made about the applicability of any model. Thus, if the results in [2-6] are in agreement with the melting model, then the silicon temperature determined by the Raman scattering method is anomalously low ( $<600^\circ\text{K}$ ), which verifies the plasma method in the opinion of the authors of [1].

At this time the overwhelming majority of researches tend towards the melting model; however, as is shown in a number of theoretical and experimental papers, the plasma effects can play a definite part, especially in the area of the prethreshold exposure modes [7].

Starting from the thermal model of annealing in this paper, we solve the problem of melting and crystallization of a semiconducting layer under the action of a nanosecond laser pulse. Utilization of a numerical method permitted taking account of temperature and spatial dependences of the optical and thermophysical semiconductor parameters as well as the actual shape of the laser pulse. Results of a computation are compared with experimental data obtained earlier in investigating the dynamics of silicon annealing by a monopulse ruby laser ( $\lambda = 0.69 \mu\text{m}$ ,  $t_e = 80 \text{ nsec}$ ) [5, 6]. The measured values of the temperature and the "lifetime" of the melt are in good agreement with the computation.

The generation of "hot" electrons and holes occurs under the effect of intense laser emission with quantum energies exceeding the forbidden-band width, and in a time on the order of  $10^{-12}$  sec these electrons and holes relax in energy with the emission of phonons. As a result of such interband relaxation, the temperatures of the electron and lattice subsystems are equilibrated. At such high excitation levels as hold for laser annealing, the Auger phenomenon plays the main role. For an electron-hole plasma with initial concentration  $10^{20} \text{ cm}^{-3}$  the effective lifetime is  $\sim 10^{-10}$  sec and the corresponding diffusion length for the nonequilibrium carriers is small compared with the degree of radiation absorption. This permits neglecting the contribution of the nonequilibrium electron-hole pairs to heat transfer.

During energy transfer from the excited carriers to the lattice, nonequilibrium phonons occur that do not succeed in relaxing completely during the pulse. However, the contribution of the nonequilibrium phonons to the heat conduction is sufficiently small and can be neglected [7].

The heat-conduction equation corresponds to a macroscopic description that is valid under conditions when the temperature changes insignificantly in the phonon mean free path. In our case this corresponds to satisfying the inequality

---

Institute of Electronics, Academy of Sciences of the Belorussian SSR, Minsk. Translated from *Inzhenerno-Fizicheskii Zhurnal*, Vol. 48, No. 2, pp. 306-312, February, 1985. Original article submitted January 4, 1984.

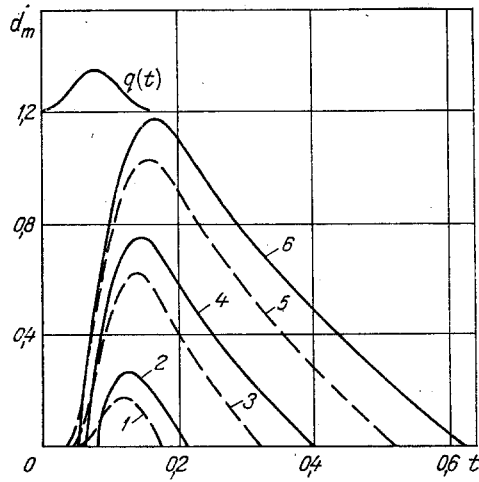


Fig. 1. Computational time dependences of the thickness of a melted layer for implanted (1, 3, 5) and monocrystalline (2, 4, 6) silicon at exposure energy densities of 1.5 J/cm<sup>2</sup> (1, 2); 2.5 J/cm<sup>2</sup> (3, 4); 3.5 J/cm<sup>2</sup> (5, 6).  $d_m$  in  $\mu\text{m}$ , and  $t$  in  $\mu\text{sec}$ .

$$\frac{k}{C\rho s} \ll \max \left\{ \alpha^{-1}, \sqrt{\frac{kt_u}{C\rho}} \right\} \quad (s \text{ is the speed of sound}).$$

Using the characteristic values of the parameters, it is easy to show that this inequality is satisfied.

Therefore, for pulses of nanosecond duration the state of the semiconductor region to be annealed can be described by a temperature field that is determined from the heat-conduction equation, while the corresponding thermophysical and optical coefficients are taken for equilibrium conditions.

In our case it is convenient to formulate the problem of semiconductor heating and melting as follows:

$$\rho(T)[C(T) + L_m\delta(T - T_m)] \frac{\partial T}{\partial t} = \frac{\partial}{\partial x} \left[ k(T) \frac{\partial T}{\partial x} \right] + \alpha(T, x)[1 - R(d_m)] q(t) \exp \left[ - \int_0^x dx' \alpha(T, x') \right], \quad (1)$$

$$\left. \frac{\partial T}{\partial x} \right|_{x=0} = 0, \quad T(x = d, t) = T(x, t = 0) = \theta,$$

$$C(T) = \begin{cases} C_s, & T < T_m, \\ C_l, & T > T_m, \end{cases} \quad k(T) = \begin{cases} k_s, & T < T_m, \\ k_l, & T > T_m, \end{cases}$$

$$\rho(T) = \begin{cases} \rho_s, & T < T_m, \\ \rho_l, & T > T_m, \end{cases} \quad \alpha(T, x) = \begin{cases} \alpha_s, & T < T_m, \\ \alpha_l, & T > T_m. \end{cases}$$

The second term in the right side of (1) describes heat liberation due to absorption of laser radiation. The coefficient of light absorption in the solid phase  $\alpha_s$  depends explicitly on the coordinate  $x$ ; the difference between the absorption coefficients of the amorphized layer and the monocrystalline substrate is thereby taken into account. In the solid phase the silicon reflection coefficient at the ruby laser wavelength is practically independent of the temperature and equals 0.35 (0.45) for the monocrystalline (amorphous) state. From the beginning of the melting, the reflectivity grows as the melt layer thickness  $d_m$  increases and reaches the value 0.72 corresponding to the melt. In specific computations below we use the computational dependence  $R(d_m)$  presented in [8].

The term with the  $\delta$  function in the left side of (1) assures continuity of the heat flux on the crystal-melt interface with the latent heat of the phase transition taken into account. The advantage of formulating the phase transition problem in the form of (1) is especially per-

ceptible when utilizing numerical methods since there is no necessity explicitly to extract the solid and liquid phase boundary in this case, and the computation can be performed by the ripple-through computation method by the ordinary difference scheme.

The method of smoothing [9, 10], whose crux is that the  $\delta$  function is approximated by a  $\delta$ -like function that is different from zero in a finite temperature interval near the phase transition point, was used to solve the problem (1). The smoothed effective coefficient of heat conduction was also introduced. In our case, the  $\delta$ -like function was approximated by a rectangular pulse whose width was chosen automatically during the computation, and in such a manner that two points of the mesh were within it.

We will consequently have a quasilinear heat-conduction equation with an effective specific heat and heat conductivity. We shall seek the solution of this equation by the method of finite differences in the domain  $0 \leq x \leq L, t \geq 0$ . Since a surface layer of several micrometers succeeds in being heated during the pulse, the quantity  $L$  can be taken very much smaller than the specimen thickness but at the same time considerably greater than the depth of heating.

Let us introduce the nonuniform mesh  $\omega_{h\tau} = \{x_i, i=0, 1, \dots, N; x_0=0, x_N=L, t_j=j\tau, j=0, 1, \dots\}$ . The partition interval along the  $x$  axis was chosen variable since the temperature gradient near the surface is substantially greater than in the bulk. Consequently, the quantity of partition points is diminished significantly, and the volume of the calculations is correspondingly reduced.

We use an implicit linear difference scheme for the numerical solution of the quasilinear heat-conduction equation. This scheme is absolutely stable, and in the class of discontinuous coefficients is apparently of first-order accuracy in the time and the coordinate [9, 10].

We have a system of  $N + 1$  linear algebraic equations

$$\begin{aligned} A_i \hat{T}_{i-1} - C_i \hat{T}_i + B_i \hat{T}_{i+1} &= -F_i, \quad i = 1, 2, \dots, N-1, \\ \hat{T}_0(1 + B_0) &= B_0 \hat{T}_1 + F_0, \\ \hat{T}_N &= 0 \end{aligned} \quad (2)$$

to find the temperature field at the time  $t_{j+1} = \tau(j + 1)$ .

The coefficients of the system (2) are expressed in terms of known values of the temperature on the previous time layer  $t_j = \tau j$  and are the following:

$$\begin{aligned} A_i &= \frac{\tau \tilde{k}(T_{i-1/2})}{\tilde{C}(T_i) h_{i-1} \bar{h}_i}, \quad B_i = \frac{\tau \tilde{k}(T_{i+1/2})}{\tilde{C}(T_i) h_i \bar{h}_i}, \quad C_i = 1 + A_i + B_i, \\ F_i &= \frac{\tau \alpha(T_i, x_i)}{\tilde{C}(T_i)} [1 - R(d_m)] q(t = t_{j+1/2}) \times \\ &\quad \times \exp \left\{ -\frac{1}{2} \sum_{k=0}^{i-1} h_k [\alpha(T_k, x_k) + \alpha(T_{k+1}, x_{k+1})] \right\} + \\ &\quad + T_i, \quad i = 1, 2, \dots, N-1, \\ B_0 &= \frac{\tau \tilde{k}(T_{1/2})}{\tilde{C}(T_0) h_0^2}, \quad F_0 = \frac{\tau \alpha(T_0, 0)}{\tilde{C}(T_0)} [1 - R(d_m)] q(t = t_{j+1/2}) + T_0, \\ \tilde{k}(T_{i \pm 1/2}) &= \frac{2 \tilde{k}(T_i) \tilde{k}(T_{i \pm 1})}{\tilde{k}(T_i) + \tilde{k}(T_{i \pm 1})}. \end{aligned} \quad (3)$$

Here  $T_i = T_i^j = T(x_i, t_j)$ ,  $\hat{T}_i = T_i^{j+1}$ ,  $h_i = x_{i+1} - x_i$ ,  $\bar{h}_i = (h_i + h_{i-1})/2$ ,  $t_{j+1/2} = \tau(j + 1/2)$ ; at initial time  $T_i^0 = \theta$ .

The difference boundary value problem (2), (3) was solved by the factorization method on a BESM-6 computer. Specific calculations were performed for the case of the effect of a

ruby laser monopulse, where two versions were examined: that of monocrystalline silicon and a 100-nm-thick amorphous layer on a monocrystalline substrate.

The range of variation of  $x$  was chosen at 26  $\mu\text{m}$  and partitioned into 400 intervals as follows:  $h_1 = 0.01 \mu\text{m}$ ,  $0 \leq i \leq 199$ ;  $h_1 = 0.04 \mu\text{m}$ ,  $200 \leq i \leq 299$ ;  $h_1 = 0.2 \mu\text{m}$ ,  $300 \leq i \leq 399$ . The spacing in the time  $\tau$  was selected at 0.2 nsec. The pulse shape was approximated by a Gauss function with 80 nsec half-width and 160 nsec duration along the base. The temperature dependence of only those quantities that depend substantially on  $T$  was taken into account in the computations. This refers to the quantities  $k_s$ ,  $\alpha_s$ , and  $C_s$  for which empirical formulas for  $(k_s, \alpha_s)$  presented in [11] and  $(C_s)$  presented in [12] were used (the quantity  $\alpha_s$  was taken to be different for the amorphous layer and the monocrystalline substrate). The dependence  $\rho_l(T)$  for the melt, for which data was taken from [13], was also taken into account in the computations. The following values were used for the remaining quantities:  $\rho_s = 2.3 \text{ g/cm}^3$ ,  $C_l = 0.97 \text{ J/g}\cdot\text{K}$ ,  $L_m = 1800 \text{ J/g}$ ,  $T_m = 1683^\circ\text{K}$ ,  $k_l = 0.585 \text{ W/cm}\cdot\text{K}$ ,  $\alpha_l = 10^6 \text{ cm}^{-1}$ .

The thermophysical parameters of the amorphous layer and the monocrystalline substrate were taken identical in the computation of the dynamics of heating and melting implanted silicon. Taking their difference into account for a pulse energy  $>1.5 \text{ J/cm}^2$  cannot substantially influence the results of the computation. Indeed, estimates show that the energy difference needed for the heating and melting of amorphous and monocrystalline silicon layers 100 nm thick is  $\sim 0.02 \text{ J/cm}^2$ , i.e., is negligible in comparison with the total absorbed energy. Hence, in the computations it would be sufficient to take into account the amorphous layer reflection and absorption coefficients that have changed in comparison with the monocrystal.

It follows from the computation (Fig. 1) that the degree of melting for  $W = 1.5 \text{ J/cm}^2$  somewhat exceeds the thickness of the ion-doped layer, i.e., the annealing threshold in the computation is close to  $1.5 \text{ J/cm}^2$ , which is in agreement with its experimental value determined earlier in [14]. Taking into account the higher  $R$  and  $\alpha_s$  of the amorphous layer as compared with the monocrystal results in nonmonotonicity in the changes in the computed velocity of the melting front motion, as well as a severalfold diminution in its initial magnitude.

The maximal temperature of the melt (Fig. 2) is achieved 20 nsec after the time corresponding to the apex of the pulse. After termination of the effect of the pulse, the surface temperature diminished to  $T_m$  and remained at this level up to termination of melt crystallization. This is verified by the results of a pyrometric investigation of the laser annealing dynamics [5, 6]; the thermal radiation of the melt reaches maximal intensity 10-15 nsec later than the peak pulse power, and the plateau corresponding to the period of melt isothermy and lasting up to the drop in the elevated reflectivity of the latter is seen clearly in the thermal radiation oscillograms.

It also follows from the computation results that the rate of surface temperature rise of the implanted silicon is retarded with the appearance of a thin melt layer. A nonmonotonic change in the velocity of surface temperature rise and of melt front motion that holds in implanted silicon and is missing in the monocrystal case is apparently due to the substantial difference (for equal  $W$ ) in radiation flux magnitudes  $(1 - R)q$  absorbed by either specimen at times when the surface temperature reaches  $T_m$ .

It can be concluded from a comparison [5] of the computed and experimental dependences of the maximal temperature of the exposed surface and the "lifetime" of the melt on the energy density (Fig. 3) that the mentioned dependences are in good enough agreement (the "lifetime" of the melt or, equivalently, the annealing time is determined by the period of elevated reflectivity of the exposed surface).

Therefore, the results of computing the dynamics of nanosecond laser annealing, obtained on the basis of a numerical solution of the Stefan problem, are in good agreement with experiment, and yield a sufficiently convincing confirmation of the melting model.

#### NOTATION

$T(x, t)$ , temperature field;  $x, t$ , coordinate and time, respectively;  $T_m$ , melting point;  $L_m$ , latent heat of melting;  $\rho_s(z)$ ,  $C_s(z)$ ,  $k_s(z)$ ,  $\alpha_s(z)$ , density, specific heat, heat conduction, and coefficient of absorption of the solid (s) and liquid (l) phases;  $R$ , coefficient of radiation reflection;  $q(t)$ , laser radiation flux density;  $d$ , plate thickness;  $\bar{C}(T)$ ,  $\bar{k}(T)$ , effective specific heat and heat conductivity;  $h_1, \tau$ , coordinate and time spacings;  $\theta$ , ini-

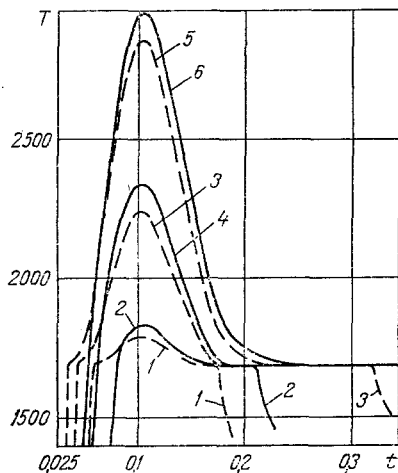


Fig. 2

Fig. 2. Computed time dependences of the surface temperature of implanted (1, 3, 5) and monocrystalline (2, 4, 6) silicon at exposure energy densities of 1.5 J/cm<sup>2</sup> (1, 2); 2.5 J/cm<sup>2</sup> (3, 4); 3.5 J/cm<sup>2</sup> (5, 6). T in °K, and t in μsec.

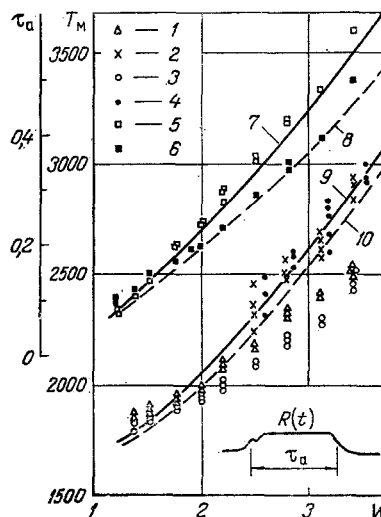


Fig. 3

Fig. 3. Comparison between the experimental [5, 6] and computed data: 1-4) experimental values of  $T_M$  determined from measuring the brightness (1, 3) and the color (2, 4) temperatures of the monocrystalline (1, 2) and implanted (3, 4) silicon surface; 5, 6) experimental values of  $\tau_a$  for both silicon, respectively; 7-10) computed dependences of the maximal surface temperature  $T_M$  (9, 10) and melt "lifetime"  $\tau_a$  (7, 8) on the exposure energy density  $W$ ; solid curves are for monocrystalline silicon, while the dashed lines are for implanted silicon.  $T_M$  in °K;  $\tau_a$  in μsec;  $W$  in J/cm<sup>2</sup>.

tial temperature;  $W$  and  $t_p$ , laser pulse energy density and halfwidth;  $T_M$ , maximal surface temperature.

#### LITERATURE CITED

1. H. W. Lo and A. Compaan, "Raman measurement of lattice temperature during pulsed laser heating of silicon," *Phys. Rev. Lett.*, **44**, No. 24, 1604-1607 (1980).
2. B. C. Stritzker, A. Pospieszczyk, and I. A. Tagle, "Measurement of lattice temperature of silicon during pulsed laser annealing," *Phys. Rev. Lett.*, **47**, No. 5, 356-358 (1981).
3. B. C. Larson, C. W. White, T. S. Noggle, and D. Mills, "Synchrotron x-ray diffraction study of silicon during pulsed-laser annealing," *Phys. Rev. Lett.*, **48**, No. 5, 337-340 (1982).
4. D. von der Linde and G. Wartmann, "Lattice temperature rise of silicon during laser annealing," *Appl. Phys., Ser. B*, **29**, No. 3, 182 (1982).
5. V. A. Pilipovich, G. D. Ivlev, V. V. Zhidkov, and V. L. Malevich, "Pyrometric measurement of the silicon temperature under nanosecond silicon annealing," *Zh. Tekh. Fiz., Pis'ma*, **9**, No. 10, 594-598 (1983).
6. V. A. Pilipovich, G. D. Ivlev, V. V. Zhidkov, and V. L. Malevich, "Temperature of implanted silicon under nanosecond laser annealing conditions," *Ion Implantation in Semiconductors and Other Materials. Abstracts of Reports of an International Conference, Vilnius, September 27-29, 1983 [in Russian], Vilnius (1983), pp. 189-190.*
7. A. V. Dvurechenskii, G. A. Kachurin, E. V. Nidaev, and L. S. Smirnov, *Pulsed Annealing of Semiconductor Materials [in Russian], Nauka, Moscow (1982).*
8. A. E. Bell, "Review and analysis of laser annealing," *RCA Rev.*, **40**, No. 3, 295-338 (1979).
9. A. A. Samarskii and B. D. Moiseenko, "Economic ripple-through computation scheme for the multidimensional Stefan problem," *Zh. Vychisl. Mat. Mat. Fiz.*, **5**, No. 5, 816-827 (1965).
10. B. M. Budak, E. N. Solov'eva, and A. B. Uspenskii, "Difference method with smoothing of coefficients to solve Stefan problems," *Zh. Vychisl. Mat. Mat. Fiz.*, **5**, No. 5, 828-840 (1965).

11. R. O. Bell, M. Toulemonde, and P. Siffert, "Calculated temperature distribution during laser annealing in silicon and cadmium telluride," *Appl. Phys.*, 19, No. 3, 313-319 (1979).
12. L. V. Gurvich, I. V. Veits, V. A. Medvedev, et al., *Thermodynamic Properties of Individual Substances. Handbook Edition in Four Volumes, Vol. 2, Book 1* [in Russian], Nauka, Moscow (1979).
13. V. M. Glazov, S. N. Chizhevskaya, and N. N. Glagoleva, *Liquid Semiconductors* [in Russian], Nauka, Moscow (1967).
14. G. D. Ivlev, "Dynamics of annealing ion-doped silicon by monopulse radiation of a ruby laser," *Pis'ma Zh. Tekh. Fiz.*, 8, No. 8, 468-472 (1982).

#### HEAT-CONDUCTION PROBLEM FOR A PLATE WITH A SQUARE CUT

Yu. M. Kolyano, V. I. Gromovyk, and Ya. T. Karpa

UDC 536.24.02

A method of determining the steady temperature field in a thin plate with a square cut is proposed on the basis of the theory of function continuation.

Consider a plate of thickness  $2\delta$  with a square cut, at the surface  $|x_1| = b$ ,  $|x_2| < b$ ;  $|x_2| = b$ ,  $|x_1| < b$  of which a heat flux  $q/2\delta$  is specified, i.e.,

$$\lambda T_{,i}|_{|x_i|=b} N(x_{i\pm 1}) = \mp \frac{q}{2\delta} N(x_{i\pm 1}), \quad i = 1, 2, \quad (1)$$

where  $N(x_i) = S_+(x_i + b) - S_-(x_i - b)$  are asymmetric functions of the cut;  $T_{,i} = \partial T / \partial x_i$ ; the subscript  $i \pm 1$  in Eq. (1) means that

$$i \pm 1 = \begin{cases} 2, & i = 1, \\ 1, & i = 2; \end{cases}$$

at infinity the temperature is zero. The cut dimension  $2b$  is commensurate with the plate thickness  $2\delta$ .

The heat-conduction equation for determining the temperature field in the given plate takes the form [1]

$$\Delta T = \kappa^2 T, \quad (2)$$

where  $\kappa^2 = \frac{\alpha}{\lambda\delta}$ ;  $\Delta = \frac{\partial^2}{\partial x_1^2} + \frac{\partial^2}{\partial x_2^2}$  is the Laplacian operator.

Introducing the function

$$\theta = TN(x_1, x_2), \quad (3)$$

where  $N(x_1, x_2) = 1 - N(x_1)N(x_2)$ , its first and second derivatives with respect to  $x_1, x_2$  take the form

$$\begin{aligned} \theta_{,i} &= T_{,i}N(x_1, x_2) - [T|_{x_i=-b-0}\delta_+(x_i + b) - T|_{x_i=b+0}\delta_-(x_i - b)]N(x_{i\pm 1}), \\ \theta_{,ii} &= T_{,ii}N(x_1, x_2) - [T_{,i}|_{x_i=-b-0}\delta_+(x_i + b) - T_{,i}|_{x_i=b+0}\delta_-(x_i - b) + \\ &+ T_{,i}|_{x_i=-b-0}\delta'_+(x_i + b) - T_{,i}|_{x_i=b+0}\delta'_-(x_i - b)]N(x_{i\pm 1}), \quad i = 1, 2, \end{aligned} \quad (4)$$

where

$$\delta_{\pm}(\xi) = \frac{dS_{\pm}(\xi)}{d\xi}; \quad \delta'_{\pm}(\xi) = \frac{d\delta_{\pm}(\xi)}{d\xi}.$$

Institute of Applied Problems of Mechanics and Mathematics, Academy of Sciences of the Ukrainian SSR, Lvov. Translated from *Inzhenerno-Fizicheskii Zhurnal*, Vol. 48, No. 2, pp. 312-315, February, 1985. Original article submitted November 29, 1983.